Spectrochimica Acta Part A: Molecular and Biomolecular Spectroscopy 115 (2013) 74–78

Contents lists available at SciVerse ScienceDirect

Spectrochimica Acta Part A: Molecular and Biomolecular Spectroscopy

journal homepage: www.elsevier.com/locate/saa

Optical properties of 1,2-diaryl benzimidazole derivatives – A combined experimental and theoretical studies

J. Jayabharathi *, V. Thanikachalam, K. Jayamoorthy

Department of Chemistry, Annamalai University, Annamalainagar 608 002, Tamilnadu, India

HIGHLIGHTS

- DFT calculation is in good agreement with single crystal XRD data.
- Steric interaction must be reduced in order to obtain larger β_0 values.
- NBO analysis elucidates the delocalization within the molecule.
- Benzimidazoles can be used as potential NLO materials.
- Charge distribution was calculated by NBO and Mulliken methods.

GRAPHICAL ABSTRACT

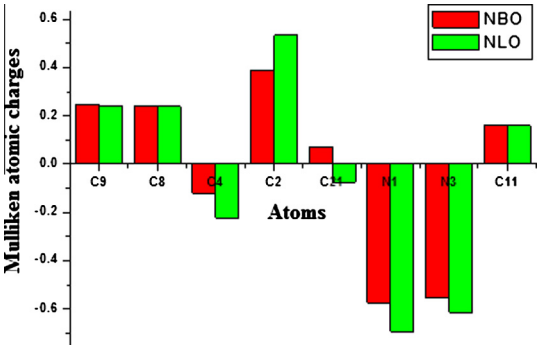

ARTICLE INFO

Article history:
Received 3 April 2013
Received in revised form 29 May 2013
Accepted 4 June 2013
Available online 17 June 2013

Keywords:
DFT/B3LYP/6-31G(d,p)
NLO
NBO
XRD
MEP

ABSTRACT

Some novel 1,2-diaryl benzimidazole derivatives have been designed, synthesized and characterized by mass, ^{1}H, ^{13}C-NMR spectral studies and single crystal XRD. The charge distribution has been calculated from the atomic charges by non-linear optical (NLO) and natural bond orbital (NBO) analyses have been calculated by abinitio method. Synthesized 1,2-diaryl benzimidazole derivatives have the largest $\mu_g\beta_0$ value and can be used as potential NLO materials. Analysis of the molecular electrostatic potential (MEP) energy surface exploited the region for non-covalent interactions in the molecule. Calculated bond lengths, bond angles and dihedral angles are found to be slightly higher than that of X-ray diffraction values of its experimental datas.

Introduction

Benzimidazole based chromophores have received increasing attention due to their distinctive linear, non-linear optical properties and also due to their excellent thermal stability in guest–host systems [1]. The imidazole ring can be easily tailored to accommodate functional groups, which allows the covalent incorporation of the NLO chromophores into polyamides leading to NLO side chain polymers [2]. Most π-conjugated systems play a major role in determining second-order NLO response [3]. Searching organic materials with non-linear optical (NLO) properties is usually concentrated on molecules with donor–acceptor π-conjugation (D-π-A) and deals with the substituent effects on the degree of π-conjugation, steric hindrance and the hyperpolarisability of the substances [4]. Nowadays there is an insufficient understanding for designing optimal NLO materials, even certain classes of D-π-A compounds were theoretically studied [5]. Searching for organic materials with nonlinear optical (NLO) properties is usually concentrated on molecules with donor–acceptor π-conjugation (D-π-A) and deals with the systematic investigation of substituent effects on the degree of π-conjugation, steric hindrance and the hyperpolarisability of the substances. Besides, geometrical arrangement of the molecules in the solid state, their interaction

* Corresponding author. Tel.: +91 9443940735.
E-mail address: jtchalam2005@yahoo.co.in (J. Jayabharathi).

1386-1425/$ - see front matter © 2013 Elsevier B.V. All rights reserved.
http://dx.doi.org/10.1016/j.saa.2013.06.001

and other physicochemical properties (e.g. strong intramolecular charge-transfer absorptions) and engineering possibilities are also important [4]. At present, there is an insufficient understanding of all influences for designing optimal NLO materials, even if the influencing factors in certain classes of D-π-A compounds were theoretically studied [5]. To quantify the push–pull effect in D-π-A compounds, bond length alternation (BLA) and out-of-plane distortions of the polarized C=C double bonds, available from X-ray studies, have been employed for a long time [6]. Alternatively, dipole moment measurements [7], bond lengths [8], barriers to rotation about the partial C=C double bonds [9] (from dynamic NMR studies), and the occupation quotients (π/π^*) [10] of the bonding (to quantify the acceptor activity) and anti-bonding orbital (to quantify the donor activities) of these C=C double bonds were adopted. Not only the push–pull effect in D-π-A compounds could be quantified, but also a linear dependence of the push–pull quotient (π^*/π) on molar hyperpolarisability of these compounds were detected. Thus, π^*/π proves to be an easily accessible, general and sensitive parameter of the donor–acceptor quality of compounds for potential NLO applications. Furthermore, we have reported the Quantum chemical analysis ((DFT/B3LYP) method with 6-311G++(d,p) as basis set) of benzimidazole derivatives **1–6** (heat of formation, geometrical structure, vibration wave numbers, NLO and NBO analysis) and the optimized geometrical parameters obtained by DFT calculation is in good agreement with single crystal XRD data. The Mulliken and NBO charge analysis were also calculated and discussed about the more basic nature of the nitrogen atom of the imidazole derivatives. The electric dipole moment (μ) and the first-hyperpolarisability (β) value of the investigated molecules have been studied by both experimentally and theoretically which reveal that they have non-linear optical (NLO) behavior with non-zero values. These chromophores possess a more appropriate ratio of off – diagonal versus diagonal β tensorial component ($r = \beta xyy/\beta xxx$) which reflects the inplane nonlinearity anisotropy since they have largest $\mu\beta_0$ values, the reported benzimidazoles can be used as potential NLO materials.

Experimental

Spectral measurements

The proton spectra at 400 MHz were obtained at room temperature using a Bruker 400 MHz NMR spectrometer. Proton decoupled ^{13}C NMR spectra were also recorded at room temperature employing a Bruker 400 MHz NMR spectrometer operating at 100 MHz. The mass spectra of the samples were obtained using a Thermo Fischer LC-Mass spectrometer in fast atom bombardment (FAB) mode. Single crystal XRD has been recorded in Agilent Xcalibur Ruby Gemini diffractometer (For 7, 8 and 12). Data collection: APEX2 (Bruker, 2008); cell refinement: APEX2 and SAINT (Bruker, 2008); data reduction: SAINT; program(s) used to solve structure: SHELXS97 (Sheldrick, 2008); program(s) used to refine structure: SHELXL97 (Sheldrick, 2008); molecular graphics: PLATON (Spek, 2009), Bruker Kappa APEXII diffractometer (for 9–11).

Non-linear optical measurements

The non-linear optical conversion efficiencies were parted using a modified set up of Kurtz and Perry. A Q-switched Nd: YAG laser beam of wavelength of 1064 nm was used with an input power of 4.1 mJ/pulse width of 10 ns, scattering geometry 90°, the repetition rate being 10 Hz, monochromater Jobin Youon Triax 550, slit width 0.5 mm, focal length of focusing lens 20 cm, PMT model number XP2262B used in Philips photonics, power supply for PMT is 1.81 KU/mA with oscilloscope Jektronix TDS 3052B.

Computational details

Quantum mechanical calculations were used to carry out the optimized geometry, NLO, NBO and HOMO–LUMO analysis with Gaussian-03 program using the Becke3-Lee-Yang-Parr (B3LYP) functional supplemented with the standard 6-31G(d,p) basis set [11]. As the first step of our DFT calculation for NLO, NBO and HOMO–LUMO analysis, the geometry taken from the starting structures were optimized and then, the electric dipole moment μ and β tensor components of the studied compounds were calculated, which has been found to be more than adequate for obtaining reliable trends in the first hyperpolarizability values.

We have reported the β_{tot} (total first hyperpolarizability) for the investigated molecules and the components of the first hyperpolarizability can be calculated using equation:

$$\beta_i = \beta_{iii} + 1/3\sum_{i\neq j}(\beta_{ijj} + \beta_{jij} + \beta_{jji}) \quad (1)$$

Using the x, y and z components, the magnitude of the first hyperpolarizability tensor can be calculated by

$$\beta_{tot}(\beta_x^2 + \beta_y^2 + \beta_z^2)^{1/2} \quad (2)$$

The complete equation for calculating the magnitude of first hyperpolarizability from Gaussian-03 output is given as follows:

$$\beta_{tot} = \left[(\beta_{xxx} + \beta_{xyy} + \beta_{xzz})^2 + (\beta_{yyy} + \beta_{yzz} + \beta_{yxx})^2 + (\beta_{zzz} + \beta_{zxx} + \beta_{zyy})^2\right]^{1/2} \quad (3)$$

All the electric dipole moment and the first hyperpolarizabilities are calculated by taking the Cartesian coordinate system (x, y, z) = (0, 0, 0) at own center of mass of the compounds.

Natural bond orbital (NBO) analysis

NBO analysis have been performed on the molecule at the DFT/B3LYP/6-31G(d,p) level in order to elucidate the intramolecular, rehybridization and delocalization of electron density within the molecule. The second order Fock matrix was carried out to evaluate the donor–acceptor interactions in the NBO analysis [12]. The interactions result is a loss of occupancy from the localized NBO of the idealized Lewis structure into an empty non-Lewis orbital. For each donor (i) and acceptor (j), the stabilization energy $E(2)$ associated with the delocalization $i \rightarrow j$ is estimated as

$$E(2) = \Delta E_{ij} = q_i \frac{F(i,j)^2}{\varepsilon j - \varepsilon i} \quad (4)$$

where q_i is the donor orbital occupancy, εi and εj are diagonal elements and F (i, j) is the off diagonal NBO Fock matrix element [13]. The larger the $E(2)$value, the more intensive is the interaction between electron donors and electron acceptors, i.e., the more donating tendency from electron donors to electron acceptors and the greater the extent of charge transfer or conjugation of the whole system.

Results and discussion

Single crystal XRD analysis

*Crystal structure of 1,2-diphenyl-1H-benzo[d]imidazole (**1**)*

1,2-Diphenyl-1H-benzo[d]imidazole is monoclinic crystal and crystallizes in the space group $C2/c$. The cell dimensions are a = 10.1878 (3) Å, b = 16.6399 (4) Å, c = 17.4959 (5) Å. ORTEP diagram of **1** presented in Fig. S1a, shows that the benzimidazole unit is close to being planar (maximum deviation = 0.0102 (6) Å) and forms dihedral angles of 55.80 (2) and 40.67 (3)° with the adjacent phenyl rings; the dihedral angle between the phenyl rings is 62.37

(3)°. Fig. S1b displays the crystal packing diagram of **1** [14]. In the crystal, one C—H···N hydrogen bond and three weak C—H···π interactions involving the fused benzene ring and the imidazole ring are observed, leading to a three-dimensional architecture.

*Crystal structure of 2-(4-fluorophenyl)-1-phenyl-1H-benzo[d]imidazole (**2**)*

2-(4-Fluorophenyl)-1-phenyl-1H-benzo[d]imidazole is monoclinic crystal and crystallizes in the space group $P2_1/n$. The cell dimensions are a = 8.7527 Å, b = 10.1342 Å, c = 17.0211 Å. ORTEP diagram of **2** presented in Fig. S2a, shows that the benzimidazole unit is almost planar [maximum deviation = 0.0342 (9) A for C6]. Fig. S2b displays the crystal packing diagram of **2** [15]. The dihedral angles between the planes of the benzimidazole and the phenyl and the fluorobenzene groups are 58.94 (3) and 51.43 (3)°, respectively. The dihedral angle between the planes of the phenyl and the fluorobenzene rings is 60.17 (6)°. Intermolecular C4—H4···F4, C7—H7···F4 and C26—H26···F4 hydrogen bonds and weak C16—H16···π and C22—H22···π interactions involving the fused benzene ring are found in the crystal structure.

*Crystal structure of 1-phenyl-2-p-tolyl-1H-benzo[d]imidazole (**3**)*

1-Phenyl-2-p-tolyl-1H-benzo[d]imidazole is orthorhombic crystal and crystallizes in the space group Pbca. The cell dimensions are a = 15.6755 (4) Å, b = 9.3509 (6) Å, c = 21.1976 (8) Å. ORTEP diagram of **3** presented in Fig. S3a, shows that the benzimidazole ring system forms dihedral angles of 28.50 (7) and 72.44 (7)° with the tolyl and phenyl rings, respectively. Fig. S3b displays the crystal packing diagram of **3** [16]. In the crystal, molecules are linked into chains along the a-axis direction by weak C—H···N interactions. The crystal structure also features C—H···π interactions.

*Crystal structure of 2-(4-methoxyphenyl)-1-phenyl-1H-benzo[d]imidazole (**4**)*

2-(4-Methoxyphenyl)-1-phenyl-1H-benzo[d]imidazole is monoclinic crystal and crystallizes in the space group P21/*c*. The cell dimensions are a = 12.3220 (3) Å, b = 7.3030 (2) Å, c = 18.2450 (3) Å. ORTEP diagram of **4** presented in Fig. S4a, shows that the 1H-benzimidazole ring forms dihedral angles of 48.00 (6) and 64.48 (6)°, respectively with the benzene and phenyl rings, which are inclined to one another by 58.51 (7)°. Fig. S4b displays the crystal packing diagram of **4** [17]. In the crystal, weak C—H···π interactions are the only intermolecular interactions present.

*Crystal structure of 2-(4-(trifluoromethyl)phenyl)-1-phenyl-1H-benzo[d]imidazole (**5**)*

2-(4-(Trifluoromethyl)phenyl)-1-phenyl-1H-benzo[d]imidazole is triclinic crystal and crystallizes in the space group P−1. The cell dimensions are a = 8.7179 (4) Å, b = 9.6796 (5) Å, c = 11.3612 (6) Å. ORTEP diagram of **5** presented in Fig. S5a, shows that the benzimidazole unit is close to being planar [maximum deviation = 0.012 (1) Å] and forms dihedral angles of 31.43 (7) and 61.45 (9)° with the 4-(trifluoromethyl)phenyl and 1-phenyl rings, respectively; the dihedral angle between these rings is 60.94 (10)°. Fig. S5b displays the crystal packing diagram of **5** [18]. In the crystal, C—H···F hydrogen bonds link the molecules into chains along the c-axis direction. The CF3 group is rotationally disordered with an occupancy ratio of 0.557 (8):0.443 (8) for the F atoms.

*Crystal structure of 2-(1-phenyl-1H-benzo[d]imidazol-2-yl)phenol (**6**)*

2-(1-Phenyl-1H-benzo[d]imidazol-2-yl)phenol is triclinic crystal and crystallizes in the space group P−1. ORTEP diagram of **6** was presented in Fig. S6a, the benzimidazole unit is close to being planar [maximum deviation = 0.0253 (11) Å] and forms dihedral angles of 68.98 (6) and 20.38 (7)° with the adjacent phenyl and benzene rings; the dihedral angle between the latter two planes is 64.30 (7)°. An intramolecular O—H···N hydrogen bond generates an S(6) ring motif. In the crystal, molecules are linked by C—H···N and C—H···O hydrogen bonds, and consolidated into a three-dimensional architecture by π–π stacking interactions, with a centroid–centroid distance of 3.8428 (12) A. Fig. S6b displays the crystal packing diagram of **6** [19]. Intramolecular hydrogen bonding from the ORTEP initiates to study the ESIPT.

Optimization have been performed by DFT at B3LYP/6-31G(d,p) using Gaussian-03. All these XRD data are in good agreement with the theoretical values (Tables S1–S6). However, from the theoretical values it can be found that most of the optimized bond lengths, bond angles and dihedral angles are slightly higher than that of XRD values. These deviations can be attributed to the fact that the theoretical calculations were aimed at the isolated molecule in the gaseous phase and the XRD results are on at the molecule in the solid state.

α key twist

The key twist, designated as α have been examined. α is used to indicate the twist of benzimidazole ring from the aromatic six-membered ring at C-2. The twist originates from the interaction of substituent at benzyl rig attached nitrogen of the benzimidazole with the substituent at junction of aldehydic ring. The present structural information allows us to further explore the correlation between structural features and fluorescent property. When the two adjacent aromatic species are in a coplanar geometry, the p-orbitals from the C—C bond connecting the two species will have maximal overlapping and the two rings will have a rigid and partial delocalized conjugation, as the result, the bond is no longer a pure single bond, as evident from the X-ray data.

Second harmonic generation (SHG) studies of 1,2-diaryl benzimidazole derivatives

Second harmonic signals of 51 (**1**), 57 (**2**), 54 (**3**), 49 (**4**), 58 (**5**) and 55 (**6**) mV was obtained for 1,2-diaryl benzimidazole derivatives by an input energy of 4.1 mJ/pulse. But the standard KDP crystal gave a SHG signal of 110 mV/pulse for the same input energy. The second order non-linear efficiency will vary with the particle size of the powder sample [20]. Higher efficiencies are achieved by optimizing the phase matching [21]. On a molecular scale, the extent of charge transfer (CT) across the NLO chromophore determines the level of SHG output, the greater the CT and the larger the SHG output.

Comparison of $\mu\beta_0$

When their dipole moment aligned in a parallel fashion the overall polarity of the synthesized 1,2-diaryl benzimidazole derivatives was small (Fig. S7). When the electric field is removed, the parallel alignment of the molecular dipole moments begins to deteriorate and eventually the benzimidazoles loses its NLO activity. The ultimate goal in the design of polar materials is to prepare compounds which have their molecular dipole moments aligned in the same direction [22].

Theoretical investigation plays an important role in understanding the structure–property relationship, which is able to assist in designing novel NLO chromophores. The electrostatic first hyperpolarizability (β) and dipole moment (μ) of the imidazole chromophore have been calculated by using Gaussian 03 package [23]. Table 1 shows the synthesized 1,2-diaryl benzimidazole derivatives have larger $\mu_g\beta_0$ values, which is attributed to the positive contribution of their conjugation.

Table 1
Electric dipole moment (μ), polarizability (α) and hyperpolarisability (β) of **1–6**.

Parameter	1	2	3	4	5	6
μ_x	−0.4087	0.2820	−0.4741	0.2376	0.9087	−0.7940
μ_y	0.8032	0.4944	0.7439	0.0939	0.1249	0.5535
μ_z	1.0823	1.0454	0.9931	0.9872	1.4069	0.7135
μ_{tot}	1.4768	1.8218	2.2110	1.3187	2.4405	2.0610
α_{xx}	253.7866	290.5813	314.3461	327.8061	331.7883	290.2289
α_{xy}	−49.9949	−57.2139	−62.1915	−55.0390	−17.6190	−56.1661
α_{yy}	119.0665	125.1516	134.8593	134.3488	124.1276	125.9119
α_{xz}	−8.5772	−5.0785	−3.5873	−2.4792	−12.3539	−4.2619
α_{yz}	12.7956	14.4184	13.9635	14.6297	−20.1380	15.5970
α_{zz}	227.6581	238.8667	246.3638	247.4461	238.9194	250.5170
$\alpha_{tot} \times 10^{-23}$	2.9665	3.2337	3.4361	3.5054	3.4325	3.2933
β_{xxx}	−158.3280	−47.4430	17.7405	22.0357	−1359.7655	30.4546
β_{xxy}	41.8472	−8.1897	−17.1877	−31.4917	−38.6190	−38.4757
β_{xyy}	−27.9548	20.0538	4.2778	8.9495	−13.6394	31.0037
β_{yyy}	42.2292	26.4870	33.9766	32.7747	−0.03635	−13.4541
β_{xxz}	65.2160	8.4763	11.6881	−41.1196	−119.1107	11.4575
β_{xyz}	−32.5731	8.7341	8.9065	13.2622	−19.0536	10.1066
β_{yyz}	58.1896	6.2045	5.1520	6.7521	20.1559	0.4994
β_{xzz}	−64.8049	22.4067	8.1889	16.1520	−130.7981	6.2343
β_{yzz}	55.0181	9.9729	12.4308	12.1062	17.9414	8.3431
β_{zzz}	53.5076	4.5970	4.2884	4.0579	231.8710	6.2315
$\beta_{tot} \times 10^{-31}$	29.1300	2.9873	4.0638	4.9778	130.4710	7.1309
$\mu \times \beta_0 \times 10^{-31}$	43.0192	5.4422	8.9850	6.5642	318.4145	14.6968

Octupolar and dipolar components of 1,2-diaryl benzimidazole derivatives

The 1,2-diaryl benzimidazole derivatives possess a more appropriate ratio of off-diagonal versus diagonal β tensorial component ($r = \beta_{xyy}/\beta_{xxx}$) which reflects the inplane non-linearity anisotropy and the largest $\mu\beta_0$ values. The difference of the β_{xyy}/β_{xxx} ratios can be well understood by analyzing their relative molecular orbital properties. The r values of 1,2-diaryl benzimidazole derivatives are −0.2643 (**1**), −0.4227 (**2**), −0.2411 (**3**), 0.4061 (**4**), −0.0100 (**5**), −1.0180 (**6**). The electrostatic first hyperpolarizabilities (β_0) and dipole moment (μ) of the chromophores have been investigated theoretically. These observed results can be explained by the reduced planarity in such chromophores caused by the steric interaction azomethine nitrogen atom. Hence, the steric interaction must be reduced in order to obtain larger β_0 values.

The β tensor [24] can be decomposed in a sum of dipolar ($^{2D}_{J=1}\beta$) and octupolar ($^{2D}_{J=3}\beta$) tensorial components, and the ratio of these two components strongly depends on their 'r' ratios. Complying with the Pythagorean theory and the projection closure condition, the octupolar and dipolar components of the β tensor can be described as:

$$\|^{2D}_{j=1}\beta\| = (3/4)\left[(\beta_{xxx} + \beta_{xyy})^2\right] + \left[(\beta_{yyy} + \beta_{yxx})^2\right] \quad (5)$$

$$\|^{2D}_{j=3}\beta\| = (1/4)\left[(\beta_{xxx} - 3\beta_{xyy})^2\right] + \left[(\beta_{yyy} + \beta_{yxx})^2\right] \quad (6)$$

The parameter ρ^{2D} $\left[\rho^{2D} = \frac{\|^{2D}_{J=3}\beta\|}{\|^{2D}_{J=1}\beta\|}\right]$ is convenient to compare the relative magnitudes of the octupolar and dipolar components of β. The observed positive small ρ^{2D} value reveals that the β_{iii} component cannot be zero and these are dipolar component. Since most of the practical applications for second order NLO chromophores are based on their dipolar components, this strategy is more appropriate for designing highly efficient NLO chromophores.

Natural bond orbital (NBO) analysis

NBO analysis have been performed for 1,2-diaryl benzimidazole derivatives at the DFT/B3LYP/6-31++G(d,p) level in order to elucidate the intramolecular, hybridization and delocalization of electron density within the molecule. The importance of hyperconjugative interaction and electron density transfer from lone pair electrons to the antibonding orbital has been analyzed [25]. Several donor–acceptor interactions are observed for the 1,2-diaryl benzimidazole derivatives and among the strongly occupied NBOs, the most important delocalization sites are in the π system and in the lone pairs (n) of the oxygen, fluorine and nitrogen atoms. The σ system shows some contribution to the delocalization, and the important contributions to the delocalization corresponds to the donor–acceptor interactions are C27—C30 → C25—C26, C27—C30 → C25—C26, C8—C10 → C9—C11, C9—C11 → C12—C13, C9—C11 → C12—C13, C12—C13 → C8—C10, C27—C31 → C24—C25, C27—C31 → C26—C29, C8—C9 → C10—C12, C26—C30 → C25—C28. The charge distribution of 1,2-diaryl benzimidazole derivatives was calculated from the atomic charges by NLO and NBO analysis (Fig. S8). These two methods predict the same trend i.e., among the two nitrogen atoms, azomethine nitrogen is considered as more basic site [26]. When compared to nitrogen fluorine atom are less electronegative in 1,2-diaryl benzimidazole derivatives [27].

Molecular electrostatic potential map (MEP) and electronic properties

MEP surface diagram (Fig. S9) is used to understand the reactive behavior of a molecule, in that negative regions can be regarded as nucleophilic centers, whereas the positive regions are potential electrophilic sites. The MEP map of synthesized benzimidazoles clearly suggests that the nitrogen and fluorine atoms represent the most negative potential region. The hydrogen atoms bear the maximum brunt of positive charge. The predominance of green region in the MEP surfaces corresponds to a potential halfway between the two extremes red and dark blue colour.

Conclusion

In this article we have reported benzimidazole based chromophores as potential NLO materials. All the compounds have been characterized by single crystal XRD. Comparison between theoretical and experimental have been done. The presence of α twist in these benzimidazoles drops the fluorescence quantum yield. The observed dipole moment and hyperpolarisability can be explained by the reduced planarity caused by the steric interac-

tion in nitrogen atom attached to benzyl ring. Hence, the steric interaction must be reduced in order to obtain larger β_0 values. DFT calculations show that molecules of higher hyperpolarizability have larger dipole moments used as potential NLO materials.

Acknowledgments

One of the authors Prof. J. Jayabharathi is thankful to DST [No. SR/S1/IC-73/2010] and DRDO (NRB-213/MAT/10-11) for providing funds to this research study. Mr. K. Jayamoorthy is thankful to DST [No. SR/S1/IC-73/2010] for providing fellowship.

Appendix A. Supplementary material

Supplementary data associated with this article can be found, in the online version, at http://dx.doi.org/10.1016/j.saa.2013.06.001.

References

[1] E.M. Across, K.M. White, R.S. Moshrefzadeh, C.V. Francis, Macromolecules 28 (1995) 2526–2532.
[2] X.R. Bu, H. Li, D.V. Derveer, E.A. Mintz, Tetrahedron Lett. 37 (1996) 7331–7334.
[3] C.W. Dirk, H.E. Katz, M.L. Schilling, L.A. King, Chem. Mater. 2 (1990) 700–705.
[4] K. Mahanalingam, M. Nethaji, P.K. Das, J. Mol. Struct. 378 (1996) 177–188.
[5] R. Koch, J.J. Finnerty, T. Bruhn, J. Phys. Org. Chem. 21 (2008) 954–962.
[6] G. Ye, W.P. Henry, C. Chen, A. Zhou, C.U. Pittman Jr., Tetrahedron Lett. 50 (2009) 2135–2139.
[7] D.M. Mitchell, P.J. Morgan, D.W. Pratt, J. Phys. Chem. *A.* 112 (2008) 12597–12601.
[8] P. Rattananakin, C.U. Pittman, W.E. Collier, S. Daebo, Struct. Chem. 18 (2007) 399–407.
[9] G. Fischer, W.D. Rudorf, E. Kleinpeter, Magn. Reson. Chem. 29 (1991) 204–206.
[10] E. Kleinpeter, A. Schulenburg, Tetrahedron Lett. 46 (2005) 5995–5997.
[11] M. Szafran, A. Komasa, E.B. Adamska, J. Mol. Struct. 827 (2007) 101–107.
[12] L. Padmaja, C. Ravikumar, D. Sajan, I.H. Joe, V.S. Jayakumar, G.R. Pettit, O.F. Neilsen, J. Raman Spectrosc. 40 (2009) 419–428.
[13] C. Ravikumar, I.H. Joe, V.S. Jayakumar, Chem. Phys. Lett. 460 (2008) 552–558.
[14] S. Rosepriya, A. Thiruvalluvar, K. Jayamoorthy, J. Jayabharathi, S.O. Yildirim, R.J. Butcher, Acta Cryst. E68 (2012) o3283.
[15] K. Jayamoorthy, S. Rosepriya, A. Thiruvalluvar, J. Jayabharathi, R.J. Butcher, Acta Cryst. E68 (2012) o2708.
[16] T. Mohandas, K. Jayamoorthy, P. Sakthivel, J. Jayabharathi, Acta Cryst. E69 (2013) o334.
[17] T. Mohandas, K. Jayamoorthy, J. Jayabharathi, P. Sakthivel, Acta Cryst. E69 (2013) o269–o270.
[18] K. Jayamoorthy, T. Mohandas, P. Sakthivel, J. Jayabharathi, Acta Cryst. E69 (2013) o244.
[19] A. Thiruvalluvar, S. Rosepriya, K. Jayamoorthy, J. Jayabharathi, S.O. Yildirim, R.J. Butcher, Acta Cryst. E69 (2013) o62.
[20] Y. Porter, K.M. OK, N.S.P. Bhuvanesh, P.S. Halasyamani, Chem. Mater. 13 (2001) 1910–1915.
[21] M.N. Bhat, S.M. Dharmaprakash, J. Cryst. Growth. 236 (2002) 376–380.
[22] D. Steiger, C. Ahlbrandt, R. Glaser, J. Phys. Chem. B 102 (1998) 4257–4260.
[23] M.J. Frisch, G.W. Trucks, H.B. Schlegel, G.E. Scuseria, M.A. Robb, J.R. Cheeseman, J.A. Montgomery, T. Vreven, K.N. Kudin, J.C. Burant, J.M. Millam, S.S. Iyengar, J. Tomasi, V. Barone, B. Mennucci, M. Cossi, G. Scalmani, N. Rega, G.A. Petersson, H. Nakatsuji, M. Hada, M. Ehara, K. Toyota, R. Fukuda, J. Hasegawa, M. Ishida, T. Nakajima, Y. Honda, O. Kitao, H. Nakai, M. Klene, X. Li, J.E. Knox, P. Hratchian, J.B. Cross, C. Adamo, J. Jaramillo, R. Gomperts, R.E. Stratmann, O. Yazyev, A.J. Austin, R. Cammi, C. Pomelli, J.W. Ochterski, P.Y. Ayala, K. Morokuma, G.A. Voth, P. Salvador, J.J. Dannenberg, V.G. Zakrzewski, S. Dapprich, A.D. Daniels, M.C. Strain, O. Farkas, D.K. Malick, A.D. Rabuck, K. Raghavachari, J.B. Foresman, J.V. Ortiz, Q. Cui, A.G. Baboul, S. Clifford, J. Cioslowski, B.B. Stefanov, G. Liu, A. Liashenko, P. Piskorz, I. Komaromi, R.L. Martin, D.J. Fox, T. Keith, M. Al-Laham, C. Peng, A. Nanayakkara, M. Challacombe, P.M.W. Gill, B. Johnson, W. Chen, M.W. Wong, C. Gonzalez, J.A. Pople, Gaussian 03, Revision C.02, Gaussian, Inc.: Wallingford, CT, 2004.
[24] S.F. Tayyari, S. Laleh, Z.M. Tekyeh, M.Z. Tabrizi, Y.A. Wang, H. Rahemi, Mol. Struct. 827 (2007) 176–187.
[25] J. Marshal, Ind. J. Phys. 7213 (1988) 659–661.
[26] P. Wang, P. Zhu, W. Wu, H. Kang, C. Ye, Phys. Chem. Chem. Phys. 1 (1999) 3519–3525.
[27] G. Wang, F. Lian, Z. Xie, G. Su, L. Wang, X. Jing, F. Wang, Synth. Met. 131 (2002) 1–5.